Seismic Pore Water Pressure Relief Wells for Gravel Column–Bed System

Franciscus Xaverius Toha

Faculty of Civil and Environmental Engineering, Institut Teknologi Bandung
CIBE Building, 5th Floor, Room 0511, Jalan Ganesha 10, Bandung 40132, Indonesia
E-mail: fxtoha@ftsl.itb.ac.id

Abstract. Liquefaction mitigation can be achieved by dissipating seismic pore pressures. The research reported in this paper elaborates the effectiveness in dissipating seismic pore pressures of a gravel bed and relief well system using gravel columns in a case study in Cilacap, Indonesia. Seismic pore pressure generation was analyzed using commonly available methods in liquefaction analysis. The evaluated pore pressures in the sand layer and gravel columns were used in a 2D dissipation analysis using finite-difference consolidation equation solutions. The results of this study showed that a simple and cost-effective relief well and gravel bed or strip system can effectively dissipate excess pore pressures in the sand layer and gravel columns to a maximum residual pore pressure below 40%, thus reducing liquefaction potential as well as protecting the foundations in the sand.

Keywords: *gravel bed; gravel columns; liquefaction; pore pressure dissipation; pore pressure generation; relief wells; residual pore pressure; stone column.*

1 Introduction

The use of gravel columns for seismic liquefaction mitigation was first developed not long after the devastating 1964 earthquakes in Alaska and Niigata. Soil reinforcement using gravel columns, also known as stone columns, was initially utilized to increase sand formation density and to facilitate dissipation of seismically induced excess pore water pressure. The inclusion of gravel columns using displacement methods reduces the liquefaction potential, as it will induce a higher density and confines pressures in the sand. Furthermore, the higher stiffness of the gravel inclusion also reduces the seismic cyclic shear stress in the sand layer. Along with the fast pore-water pressure dissipation in the gravel column due to its high permeability, the three combined effects of the gravel column effectively reduce the liquefaction potential. Comprehensive reports of seismic performance of sites with gravel columns have been presented by Mitchell and Huber [1], Dobson [2], Mitchell and Wentz [3], Hayden and Baez [4], Hausler and Koelling [5], and more recently by Young, Gibson and Newby [6], as well as Mahoney and Kopec [7].

Received November 7th, 2016, Revised February 20th, 2017, Accepted for publication February 28th, 2017.
 ISSN: 2337-5779, DOI: 10.5614/j.eng.technol.sci.2017.49.1.4

Typically, the gravel column system for liquefaction mitigation consists of vertical gravel columns, a horizontal gravel bed or strip, and some vertical relief wells to the ground surface. As shown in Figure 1, the gravel-column top ends at the structure's base slab or pile caps, usually located several meters below the ground surface. To enable seismic excess pore pressure dissipation through the gravel columns, a gravel bed or strip is provided to convey dissipation in the horizontal direction from the top of the columns to points of release to the atmosphere. Vertical pressure relief wells are needed to allow dissipation from the gravel bed or strip to atmospheric pressure at the ground surface. The gravel columns' diameter, spacing and depth are designed to limit the increase of excess seismic pore pressure in the surrounding sand layers. The gravel bed and relief wells must have a higher pore pressure dissipation rate during earthquakes, such that undesirable pore pressure build-up in the sand and gravel columns is prevented.

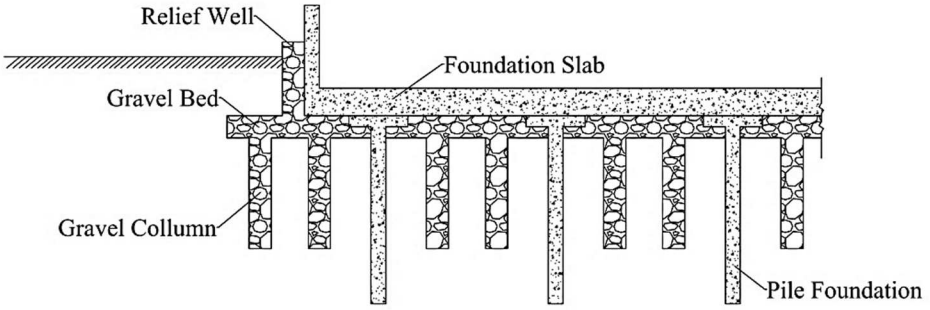

Figure 1 Typical gravel column–bed system.

In this paper, estimation of seismic excess pore pressure generation within sand based on widely accepted procedures is briefly described. The initial pore pressure in the gravel columns was conservatively assumed to be equal to what is generated in the sand. Furthermore, using a simplified two-dimensional (2D) model, the rate of pore pressure dissipation from the gravel columns in the gravel bed through the relief wells was evaluated. The pore pressure dissipation at the sand layer and gravel bed interface was conservatively ignored in the 2D model. The permeability of the vertical relief wells was assumed to be equal to that of the gravel bed, as in practice this can easily be achieved by selecting coarser aggregates for the relief wells.

A case study was conducted at a construction site at the Cilacap Refinery. The research was focused on the performance of a gravel bed and relief well system as part of an integral gravel column, gravel bed and relief well system for

liquefaction mitigation. Elaboration of the gravel column configuration, i.e. diameter and spacing based on the properties of the sand, is not included in this paper. Instead, the generated pore pressures due to cyclic shear stress in the sand layer, based on the seismic input motions, were applied as the generated pore pressures at the gravel column points within the gravel bed.

Details of the research are presented in two major parts. The first one is a detailed evaluation of the pore pressures generated in the sand layer and gravel columns during relevant input seismic events for the selected foundation at the Cilacap project, considering the in-situ sand parameters. The second part deals with the dissipation of the generated pore pressures by the prevailing configuration of gravel bed and relief wells simultaneously with pore pressure generation in the sand layer and gravel columns. A dissipation study as reported in Section 3, has not been conducted previously, particularly concerning a gravel bed and relief well system. This salient feature of the research contributes a quantitative scientific approach to the engineering aspects of the gravel column system for liquefaction mitigation.

2 Seismic Pore Pressure Generation

At the Cilacap project site, the generated seismic excess pore pressure within the sand layer with gravel columns was evaluated using the following procedure. Selected input accelerograms from a seismic hazard study were used to obtain a history of the cyclic shear stress ratio, τ_c/σ_v'. Effects of sand layer densification and gravel column effects in the reduction of cyclic shear stress ratio were included, but these effects may or may not be significant, as reported by Toha [8]. Reduction due to gravel column bending and shear stiffness, as suggested by Baez and Martin [9] and by Goughnour and Pestana [10] were considered. Analysis and field experimental data by Toha [8] indicate that cyclic shear stresses reduction in the sand layer eached 27% to 44%. Considering the controversy on this reduction, see for example Rayamajhi *et al.* [11], the minimum amount of reduction was applied in this research.

The τ_c/σ_v' history was divided into finite pore pressure generation time steps, Δt_s, where each time step contains at least one peak. For each peak, the corresponding τ_c/σ_v' was used to assess the number of cycles to liquefaction in the sand, N_l, following De Alba, Seed and Chan [12] for the Cilacap sand relative density, D_r, of 50%, and with membrane penetration effects included. Within each Δt_s, the sum of $(0.5/N_l)$ values for each peak and cyclic shear stress ratio was added to the residual $\Sigma(N/N_l)$ at the end of the previous dissipation process. Then, the updated $\Sigma(N/N_l)$ was used to assess the generated excess pore pressure, Δu, by De Alba, Chan and Seed [13], Seed, Martin and Lysmer [14],

as well as Seed and Booker [15]. The Δu was assumed to increase linearly for each sub time step within Δt_s. In the 2D model used, it was assumed conservatively that the excess pore pressure developed within the sand layer and the gravel column was equal and uniform throughout the vertical cross sections. Dissipation of pore pressures within Δt_s was done using a finite-difference method, with pore pressure dissipation time steps, Δt, as sub time steps.

A site-specific seismic study was conducted for the case-study site in 2012 by Sengara [16]. From the results of the de-aggregation analysis, the recommended input accelerations (7 sets, i.e. *212V5090, TCU120-N, TCU089-V, ABY090, FER-T1, CUC090,* and *A-SON-UP*) were scaled to a *PGA* of 0.275 g. An earthquake significant duration, $D_{5\text{-}95}$ (around 48 seconds), was adopted based on Abrahamson and Silva [17], for earthquake magnitude M = 8.03, and site to source distance r = 96.82 km. The site-specific seismic study by Sengara [16] does not provide recommended input accelerations for $D_{5\text{-}95}$. In this research, the duration of the earthquake was adjusted by linearly proportioning the time scale to the $D_{5\text{-}95}$ ratios. The τ_c/σ_v' history was then obtained from Eq. (1):

$$\frac{\tau_c}{\sigma_v'} = \frac{a}{g} \quad \frac{\sigma_v}{\sigma_v'} r_d \tag{1}$$

where a is the acceleration, g is the gravitational acceleration, σ_v/σ_v' is the total to effective vertical stress ratio, and r_d is the stress reduction factor according to Seed and Idriss [18]. In this case study, r_d was set to 0.96.

All seven calculated τ_c/σ_v' histories in the Cilacap case study [19], shown in Figure 2, were used to obtain the Δu in the sand layer at the start of each Δt_s for the first quadrant of the gravel-bed area of the RX-RG Reactor Tower structure shown in Figure 3. During the design stage of the case study early in 2012, a 500-year return period was adopted to obtain a *PGA* value of 0.275 g. A maximum τ_c/σ_v' value of 0.379 was used. After the design of the Cilacap case study was completed, an update of SNI 1726 was issued in mid-2012 [20] in which the liquefaction analysis requirement was increased to an MCE_G with a 2500-year return period. This new requirement would result in an increase of the maximum τ_c/σ_v' value to 0.461. There was no additional site-specific seismic analysis for a 2500-year return period for the Cilacap project, so the analysis of pore pressure generation and dissipation for this earthquake was done using the above 7 sets of input motions by scaling only the maximum accelerations.

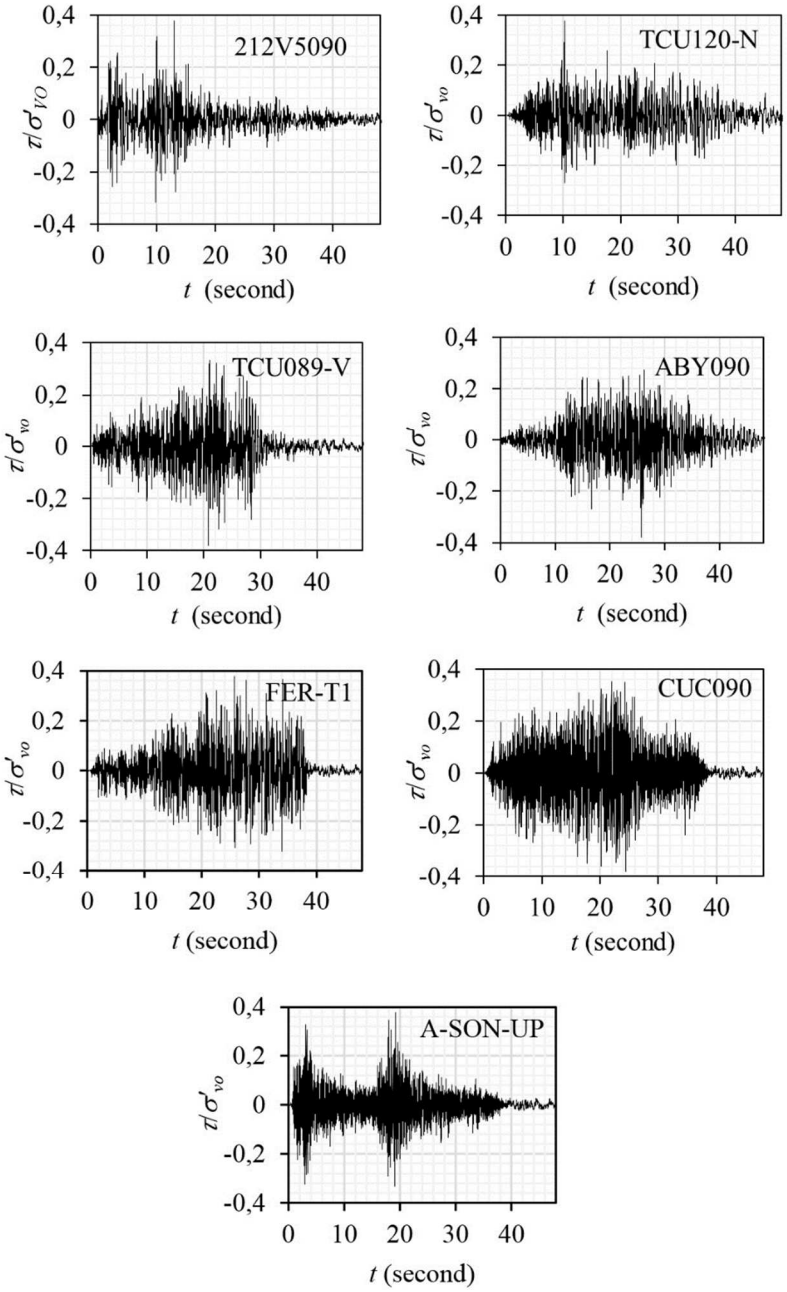

Figure 2 Cyclic shear stress ratio, τc/σv' history.

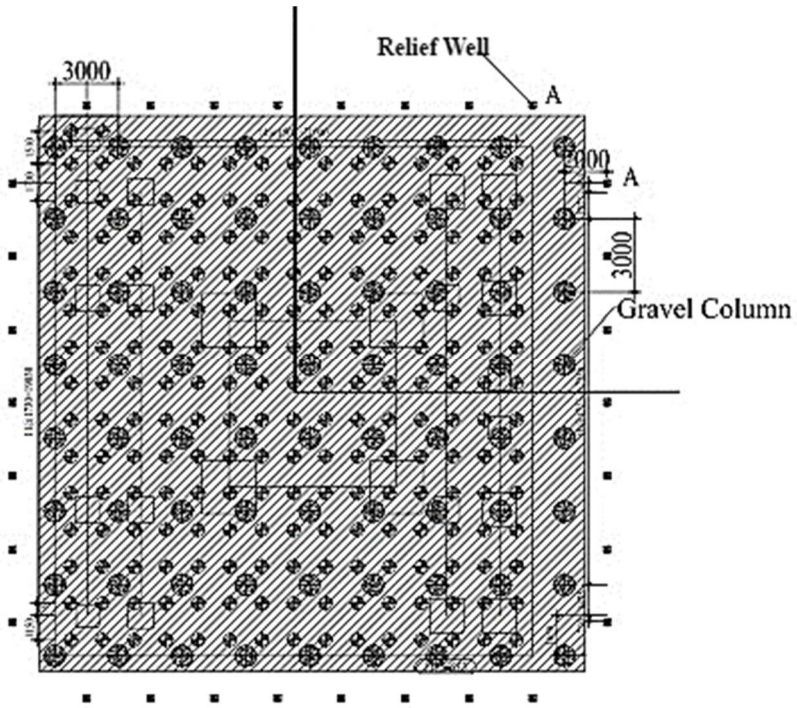

Figure 3 RX-RG Tower gravel column layout in Cilacap [18].

After assessing the generated pore pressures, the dissipation was processed as described in Section 3 of this paper for every point on the grid. The generated and residual pore pressures at the center of the gravel bed, Point O, are used here as the most critical pore pressures during the process.

After evaluating Δu, within Δt_s, Δu was subdivided into equal stages of generated excess pore pressures, u_o, as follows:

$$u_o = \frac{\Delta t}{\Delta t_s} \Delta u \tag{2}$$

where Δt is the dissipation time step, which should be small enough to ensure numerical stability in the computations. Among the seven τ_c/σ_v' histories, *CUC090* represents the most critical history in terms of pore pressure generation. The calculated u_o at *Point O* during the *CUC090* event is shown in Figure 4 for the entire seismic event and detailed for a selected period, where Δt_s = 0.049 seconds and Δt, = 0.0014 seconds.

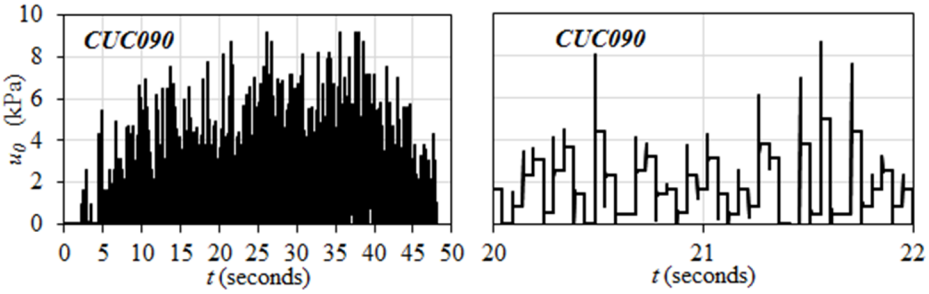

Figure 4 Generated excess pore pressure, u_o, during CUC090 history.

Although it seems that u_o values shown in Figure 4 are relatively small compared to the total stress, σ_v, the value of u_o multiplied by $\Delta t_s/\Delta t$ will result in a high generated pore pressure within Δt_s. Without dissipation, $\Sigma\ u_o$ accumulation would far exceed σ_v, as can be seen from Figure 5. In fact, since there are some τ_c/σ_v' values above 0.3, which will result in $2N_l < 1.0$ according to de Alba, *et al.* [12], the absence of the gravel column-bed and relief well system would have induced a liquefied condition.

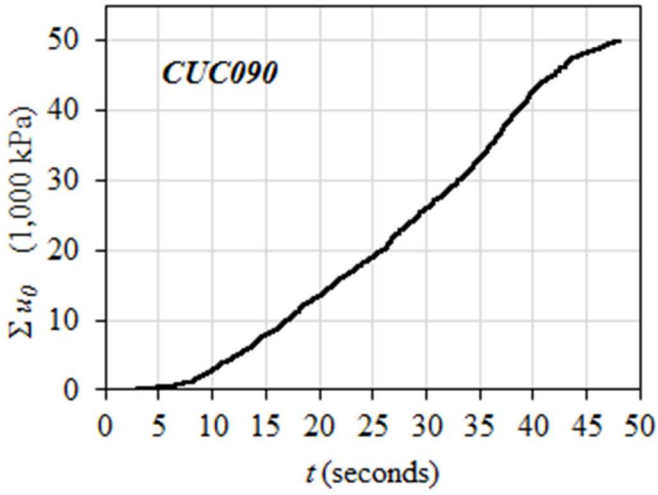

Figure 5 Accumulation of u_o during CUC090 history.

However, since Δt was smaller than the half period of the larger peaks, each u_o increase (as part of Δu) during Δt was partially or entirely dissipated at the same time by the gravel column and bed as well as the relief well system, as shown in detail in Figure 6 for the *CUC090* event at the 26-27 seconds time slot, where the darker lines represent u and the lighter lines represent the residual pore pressure, u_{res}, after dissipation.

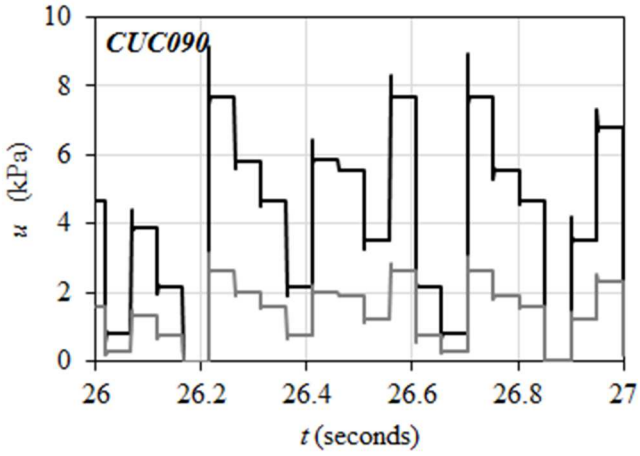

Figure 6 Details of pore pressure generation and dissipation during Δt.

The higher the dissipation rate of the system, the smaller u_{re} at the end of Δt, hence at the next Δt, the initial excess pore water pressure will also be smaller than σ_v. The details of the dissipation analysis are described in Section 3 of this paper.

3 Pore Pressure Dissipation

Dissipation of seismic excess pore pressure in sand layers by gravel columns is most commonly evaluated using the Seed and Booker method [15] for a given configuration of gravel column diameter, length and spacing. The gravel column material is generally assumed to be a free-draining material with relatively high permeability values compared to that of sand. Analysis of pore pressure distribution within the sand layer with gravel column inclusions was not done in this research. Instead, a conservative average pore pressure in the sand layer, with the same value as the evaluated generated pore pressure as described in Section 2, was assumed to prevail within the sand layer and the vertical gravel columns. Furthermore, the pore pressure in the gravel column was assumed to be constant with depth. As the gravel column must dissipate the pore pressures, it is necessary that the gravel column and its downstream dissipation system, i.e. the gravel bed and relief wells, must dissipate the pore pressures faster than the build-up rate.

In practice, the required gravel column configuration, as well as the necessary gravel bed thickness and spread, rarely interfere with the foundation and other structures. The vertical dissipation structures, i.e. the relief wells at the top of the gravel column–bed system, however, may coincide with the foundation

elements and other underground facilities, as the foundation slab often covers a large area, such that the dissipation must be done by placing the relief wells at a significant distance from the excess pore pressure points. Opening the base slab for the pore pressure relief wells is usually unacceptable, due to its effect on the base slab's structural integrity and possible ground contamination from undesired water leaks above to slab.

A typical detail of a pore pressure relief well for a gravel column–gravel bed system, is shown in Figure 7. The pore pressure relief well is provided primarily to dissipate the pressure in the pore water within the gravel bed and gravel column, such that the pore pressure build-up in the sand layer can be controlled. The relief well does not require a large flow discharge capacity, as water flow can be allowed to occur after an earthquake. Based on field application of relief wells during various projects, it is best to use compacted gravel or crushed rock aggregates. The gravel material should be coarser than the gravel-bed material, such that the pressure gradient herein is negligible. The top 300 mm can be removed and cleaned periodically to ensure that the well is always exposed to atmospheric pressure.

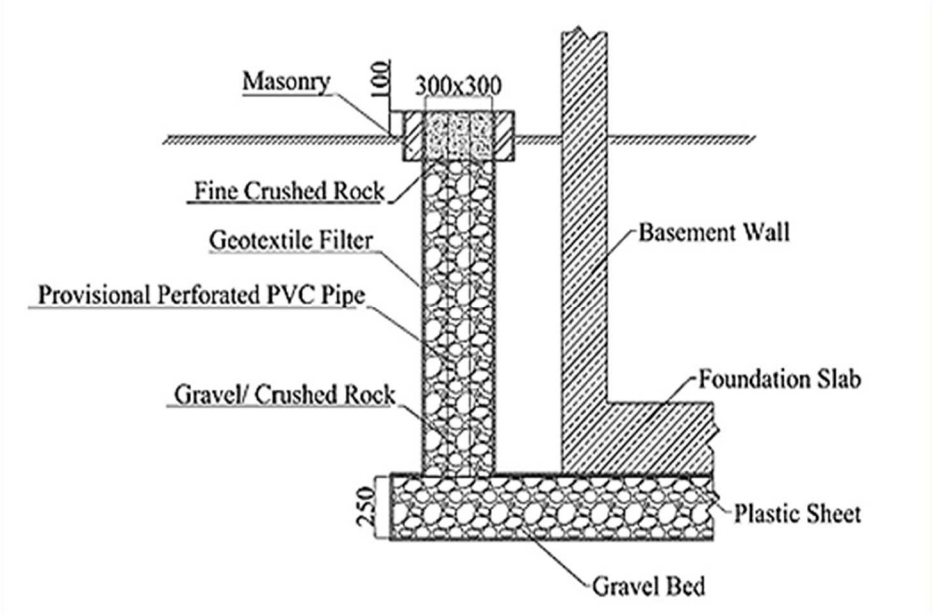

Figure 7 Typical cross section of relief well.

An optional feature is to provide a backflow permeable PVC pipe to pump water into the well in order to open the voids that may be clogged by finer material migration through the filter due to water flowing into the well. If the relief-well top is situated at the highest site elevation, water from and into the

well clogging the aggregate voids will be very rare. Preliminary trial pumping from inside the well showed that there was no significant clogging in the gravel of the relief well after several minutes of repeated cycles of intermittent pumping.

The 2D consolidation governing equation used for pore pressure dissipation analysis in the gravel bed and relief well system shown in Figures 3 and 7, is as follows:

$$c_v\left(\frac{\partial^2 u}{\partial x^2}+\frac{\partial^2 u}{\partial y^2}\right)=\frac{\partial u}{\partial t} \tag{3}$$

where u is the excess pore pressure, c_v is the 2D coefficient of consolidation, x, y and t are the spatial coordinates and time variable, respectively. In an explicit finite difference scheme with equal grid spacing in the x and y directions, Eq. (3) can be written as:

$$u_{i,j,t+1}=u_{i,j,t}\left(1-4\Delta T\right)+\Delta T\left(u_{i+1,j,t}+u_{i,j+1,t}+u_{i-1,j,t}+u_{i,j-1,t}\right) \tag{4}$$

with $\Delta T = c_v\,\Delta t/\Delta x^2 = c_v\,\Delta t/\Delta y^2$, where Δt are the pore pressure dissipation time steps, while Δx and Δy are the grid spacings in the x and y directions, respectively. For the Cilacap [19] case study, c_v was 5 m^2/sec, Δx and Δy were 1 m. In Figure 3, the gravel column diameter and spacings are 1 m and 3.5 m, respectively.

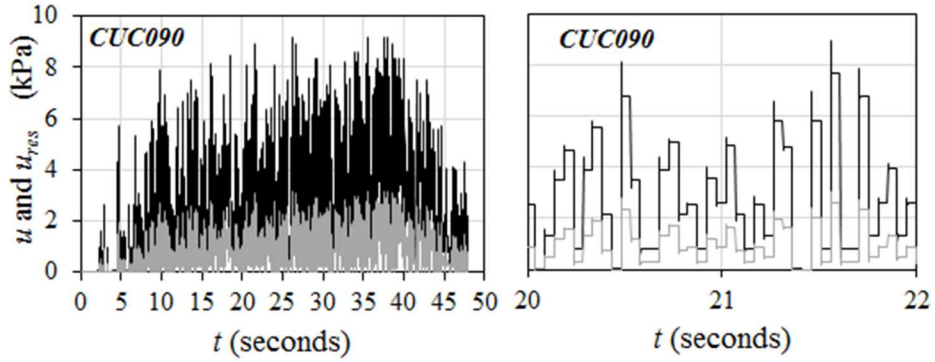

Figure 8 Initial and residual pore pressures for each Δt.

At the relief-well pressure points, u = 0 was assumed at all t values. At the beginning of Δt, u_o from Eq.(2) was added to the residual pore water pressures from the previous Δt at the gravel column points only. Subsequently, u_o was dissipated accordingly using finite-difference Eq. (4). ΔT = 0.007 was adopted

in the computations. The pore pressures at *Point O* from the analysis are shown for the *CUC090* input history in Figure 8, where the darker lines are the initial pore pressures, u, at the beginning of each Δt, and the lighter lines are the residual pore pressures, u_{res}, after dissipation at the end of the Δt. The results show that the pore pressures were relatively low compared to the total vertical stress, σ_v, meaning that the gravel bed and relief well system kept the pore pressures to well below liquefaction condition.

In order to obtain better insight into the gravel bed and relief well system's effectiveness during the *CUC090* event, selected values of the ratio of the generated pore pressure, u_o, to the dissipated pore pressure, u_{dis}, throughout the event, were plotted in Figure 9. The u_o values were determined using the theory and method as described in Section 2. The dissipated pore pressure, u_{dis}, i.e. the difference between the pore pressure at the beginning of each Δt and the pore pressure after dissipation at the end of Δt, was assessed using the finite-difference method according to Eq. (4) in this section.

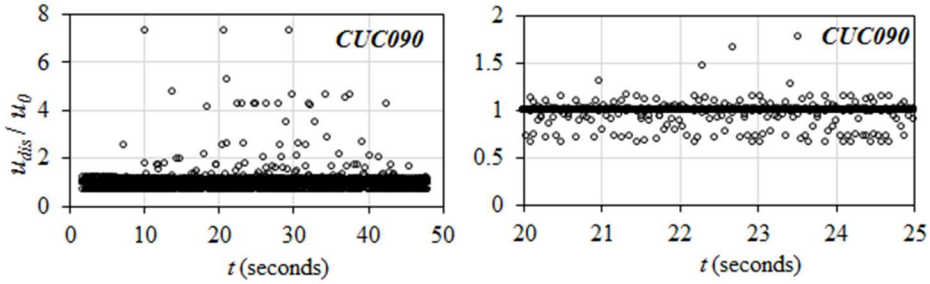

Figure 9 Ratio between dissipated pore pressure, u_{dis}, and generated pore pressure, u_o.

The u_{dis}/u_0 values were mostly around 1.0, as indicated by the intense overlapping of data points, both during the entire seismic event, as well as during the sampled high τ/σ_v' peaks between 20 to 22 seconds. This means that throughout the entire event, as well as during high τ/σ_v' occurrence, the gravel bed and relief well system managed to dissipate the generated pore pressures effectively.

Presumably, at higher values of u_o, as the dissipation capacity of the gravel bed and relief well system remains the same, the u_{dis}/u_o ratio is expected to become smaller. Figure 10 also demonstrates that for most of the generated pore pressures, u_o, dissipation occurred instantaneously in the gravel bed and relief well system, as the u_{dis}/u_o ratio values were also mostly around 1. The $u_{dis}/u_o >$ 1.0 values at $u_o < 2$ kPa demonstrate that the gravel bed and relief well system

often dissipated the residual pore pressure from the previous dissipation time step as well, especially when the subsequent generated pore water pressure, u_o, was small. Figure 10 shows that the average dissipation of the RX-RG Tower configuration was about 86% with a scatter of 30%, meaning that maximum u_{res} was only about 14% of the generated pore pressure. A slight reduction trend of u_{dis}/u_o occurred when the generated pore pressure increased.

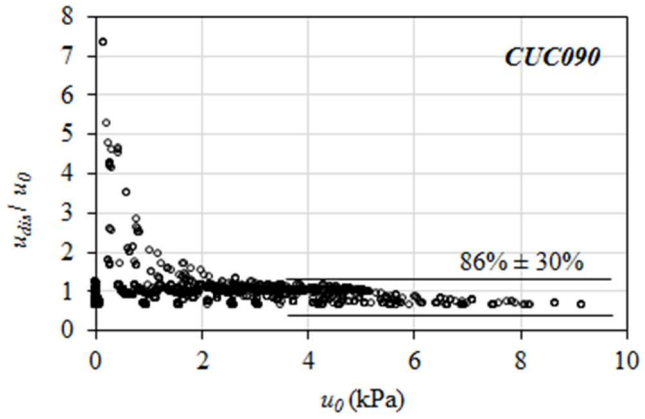

Figure 10 Ratio between dissipated pore pressure, u_{dis}, and generated pore pressure, u_o, for related u_o.

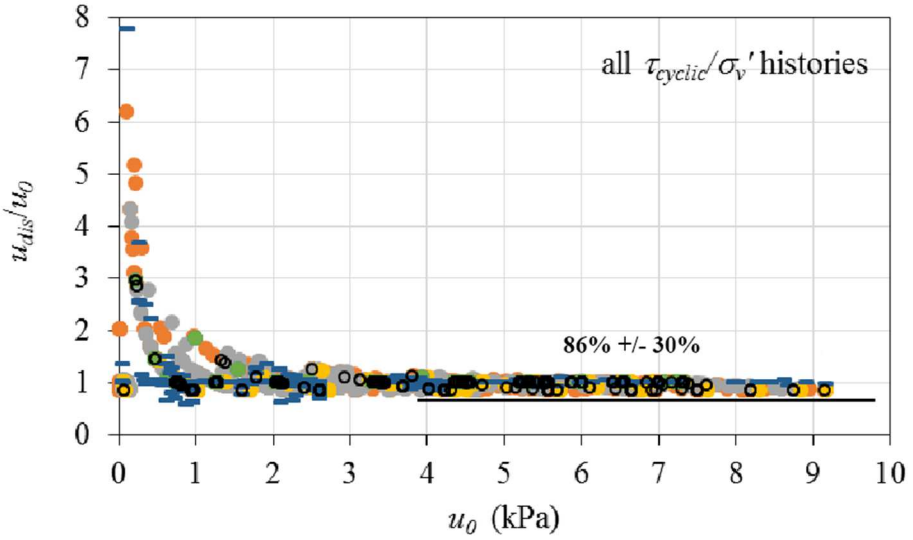

Figure 11 Dissipated, u_{dis}, to generated, u_o, pore pressure ratio for various τ_c/σ_v' histories.

The six other τ_c/σ_v' from different seismic input motions, as shown in Figure 2, also produced similar pore pressure dissipation, as shown in Figure 11, in which the same theoretical background and analysis as described in Section 2 were used to develop u_o. Eq.(4) was also used for the dissipation analysis to obtain u_{dis}. Although the selected histories developed from de-aggregation analysis in the site-specific study were intended to provide a varying seismic response, it appears that due to the large dissipation capacity of the gravel bed and relief wells, u_{res} remains essentially uniform, even though the input motions were distinctly different. The average dissipation was also 86% ± 30%.

The results from the Cilacap [19] case study show that the provided gravel bed and relief well system had a dissipation rate more than what is required by the the generated pore pressure. In this research, a more severe condition was analyzed while the engineering works for the case study were being performed, where the seismic design criteria were adjusted from the prevalent seismic code in early 2012 to the present SNI 1726 03 2012 seismic code requirement [20]. Because of the increase of the return period from 500 years to 2500 years, the PBA = 0.275 g was increased to MCE_G = 0.461 g. The same 7 earthquake input motions, scaled maximum acceleration and unscaled duration were used in the analysis. The use of an unscaled earthquake duration with an increased acceleration will increase the likelihood of liquefaction if the larger earthquakes have slower pore pressure generation rates. Data for larger earthquakes were not available at the time of conducting this research. Furthermore, a deliberately more severe relief well configuration was imposed by reducing the number of relief wells in Figure 3 to only two Point A relief wells at the most distant corner from the center of the gravel bed, Point O, such that it was expected that the pore pressure dissipation process would become much less favorable. The gravel material parameters were adjusted in the analysis by reducing the permeability to the minimum typical value, so that the coefficient of consolidation during dissipation, c_v, was reduced to only about 0.8 m^2/second. Table 1 summarizes the comparison between the design soil parameters for the Cilacap project and the least favorable parameters in the additional analysis.

Table 1 Parameters in Cilacap case study and least favorable case.

Parameters	Cilacap Case Study	Least Favorable Case
Earthquake return period	500 yrs.	2500 yrs.
PGA/MCE_G	0.275 g	0.461 g
Earthquake duration	48 sec.	48 sec.
Permeability, k	0.00235 m/sec	0.00046 m/sec.
Young's Modulus, E	30 MPa	30 MPa
Poisson's Ratio, ν	0.2	0.1
c_v	5 m^2/sec	0.8 m^2/sec.

Using the same model as described in Section 2, the generated pore pressures were processed, and subsequently, using the dissipation analysis from Section 3, the results of the dissipation analysis for all seven $\tau_c/\sigma_{v'}$ histories were imposed on the least favorable gravel bed and relief well configuration, as shown in Figure 12. In the least favorable case analysis, only the input motions were adjusted by scaling the peak accelerations. The selected input motions and duration of the earthquake were not adjusted, as there were no 2500-year site specific seismic hazard studies available at the time the Cilacap design was made.

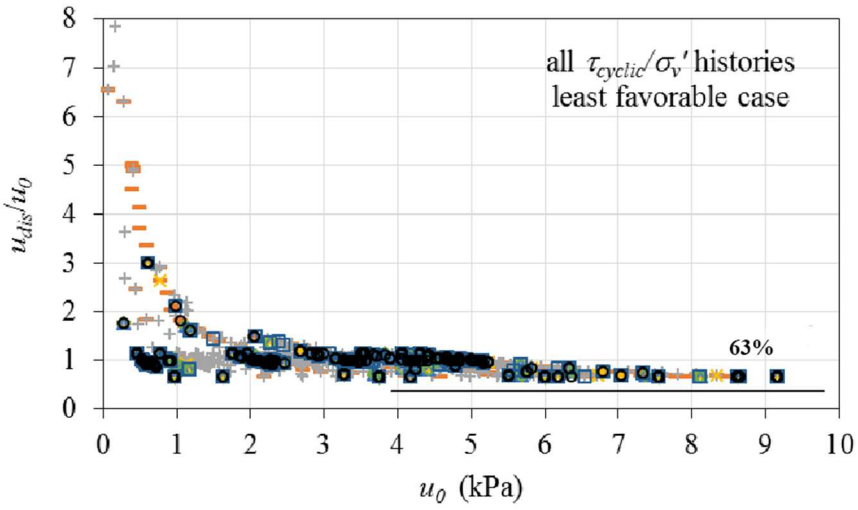

Figure 12 Pore pressure ratio under least favorable conditions.

The magnitude of generated pore pressures, u_o, were similar as in the Cilacap case study, however, since there were higher peaks of $\tau_c/\sigma_{v'}$ and the dissipation rate was reduced substantially, the u_{dis} values, approximately 63%, were relatively lower, hence resulting in a maximum residual value u_{res} of 37% of the generated pore pressure.

In the Cilacap case study, the gravel columns were designed to limit the pore pressure build-up within the sand layer to less than 40% of the total stress, such that the reduction in the axial and lateral pile capacities, footing bearing capacities, and seismic deformations were still within reasonably good performance limits. This practice followed the full-scale field test results by Ashford, *et al.* [21], where the blast-induced pore pressure ratios remained below 40% and the lateral stiffness of the piles in the treated sand increased 2.5 to 3.5 times that of the system in liquefied soil. With a maximum residual pore

pressure ratio of 37%, the general performance of the gravel column–bed and relief well system under least favorable conditions was still within acceptable boundaries. Therefore, it can be concluded that the system can be applied without necessarily imposing rather restrictive material requirements and difficult construction methods. Even a low permeability and minimum compaction efforts of the gravel would provide sufficient dissipation of the seismic pore pressures from maximum earthquakes (MCE_G) and a limited quantity of relief wells. In practice, the application of a gravel column–bed and relief well system can easily be configured economically by setting a limit on the residual pore pressures, and hence establishing the gravel column diameter and spacing, the gravel bed layout and thickness, as well as the relief well configurations.

4 Conclusions

This research elaborated the performance of a gravel bed and relief well system in conjunction with gravel columns in efforts to mitigate liquefaction potential in susceptible sand layers during large seismic events in a project at the Cilacap Refinery. The research results indicated that gravel bed and relief wells can easily dissipate the generated pore pressures within the sand layer and gravel or stone columns. Most of the time, the dissipation rate is faster than the build-up rate, such that the controlled pore pressure build-up as established for the gravel or stone columns can easily be achieved without impedance to the dissipation from the gravel columns to the open atmosphere. The gravel bed and relief wells do not require a very high permeability, high compaction efforts or numerous relief wells, as the research has shown that lower-bound permeability, standard compaction efforts and a limited number of relief wells will dissipate the pore pressures within the limits of an acceptable performance level of the gravel columns. Practical aspects and details of the gravel bed and relief well system based on various field experiences were described in this paper.

Acknowledgements

The author thanks PT Adhi Karya (Persero) for the permission to use the data from the Cilacap Refinery Project. The continued assistance from Fendy Setiawan and Andika Suparto in the later stages of the computer application development for the dissipation analysis is greatly appreciated.

Nomenclature

a	=	acceleration
c_v	=	coefficient of consolidation
$D_{5\text{-}95}$	=	earthquake significant duration
D_r	=	relative density

g	=	gravitational acceleration
M	=	earthquake magnitude
MCE_G	=	maximum considered earthquake geometric mean
N	=	number of cycles
N_l	=	number of cycles to liquefaction
PGA	=	peak ground acceleration
r	=	earthquake distance
r_d	=	stress reduction factor
t	=	time
u	=	excess pore water pressure
u_o	=	generated excess pore water pressure during Δt
u_{dis}	=	dissipated excess pore water pressure
u_{res}	=	residual excess pore water pressure
x	=	spatial coordinate
y	=	spatial coordinate
T	=	time factor
Δt	=	pore pressure dissipation time step
Δt_s	=	pore pressure generation time step
Δu	=	generated excess pore pressure during Δt_s
σ_v	=	vertical total stress
σ_v'	=	vertical effective stress
τ_c	=	cyclic shear stress

References

[1] Mitchell, J.K. & Huber, T.R., *Performance of a Stone Column Foundation*, Journal of Geotechnical Engineering, ASCE, **111**(2), pp. 205-223, 1985.

[2] Dobson, T., *Case Histories of the Vibro Systems to Minimize the Risk of Liquefaction, Soil Improvement – a Ten Year Update,* Welsh, J.P. (ed.), ASCE Geotechnical Special Publication, **12**, pp.167-183, 1987.

[3] Mitchell, J.K. & Wentz, F.J., *Performance of Improved Ground during the Loma Prieta Earthquake,* University of California, Berkeley UCB/EERC Report 91/12, 1991.

[4] Hayden, R.F. & Baez, J.I., *State of Practice for Liquefaction Mitigation in North America*, International Workshop on Remedial Treatment of Liquefiable Soils, Tsukuba Science City, Japan, July 4-6, 1994.

[5] Hausler, E.A. & Koelling, M., *Performance of Improved Ground during the 2001 Niscqualli Earthquake,* 5th International Conference on Case Histories in Geotechnical Engineering, NY, USA, April 13-17, Paper No. 327, 2004.

[6] Young, R., Gibson, M. & Newby, G., *Seismic Performance of Ground Improvements on Christchurch Southern Motorway,* Australian

Geomechanics, Australian Geomechanics Society, **47**(4), December 2012.

[7] Mahoney, D.P. & Kupec, J., *Stone Column Ground Improvement Field Trial: A Christchurch Case Study,* Proc. New Zealand Society for Earthquake Engineering Conference, Paper No. O79, March 2014.

[8] Toha, F.X., *Increase of In-Situ Measured Shear Wave Velocity in Sand with Displacement Pile and Stone Column Inclusions,* Jurnal Teknik Sipil FTSL ITB, **24**(1), 2017.

[9] Baez, J.I. & Martin, G.R., *Advances in the Design of Vibro-Systems for Improvement of Liquefaction Resistance,* Proc. Symposium on Ground Improvement, Canadian Geotechnical Society, Vancouver, 1993.

[10] Goughnour, R.R., & Pestana, J.M., *Mechanical Behavior of Stone Columns under Seismic Loading,* Proc., 2nd International Conference on Ground Improvement Techniques, CI-Primer, Singapore, pp. 157-162, 1998.

[11] Rayamajhi, D., Ashford, S.A., Boulanger, R.W. & Elgamal, A., *Dense Granular Columns in Liquefiable Ground: I: Shear Reinforcement and Cyclic Stress Ratio Reduction,* Journal of Geotechnical and Geoenvironmental Engineering, ASCE, **142**(7), Paper No. 04016023, 2016

[12] De Alba, P., Seed, H.B. & Chan, C.K., *Sand Liquefaction in Large Scale Simple Shear Tests*, Journal of the Geotechnical Engineering Divison, ASCE , **102**(9), pp. 909-927, 1976.

[13] De Alba, P., Chan, C.K. & Seed, H.B., *Determination of Soil Liquefaction Characteristics by Large-Scale Laboratory Tests*, Report No. EERC 75-14, Earthquake Engineering Research Center, University of California, Berkeley, 1975.

[14] Seed, H.B, Martin, P.P. & Lysmer, J., *The Generation and Dissipation of Pore Water Pressures during Soil Liquefaction,* Report No. EERC 75-26, Earthquake Engineering Research Center, University of California, Berkeley, 1975.

[15] Seed, H.B. & Booker, J.R., *Stabilization of Potentially Liquefiable Sand Deposits Using Gravel Drains*, Journal of the Geotechnical Engineering Division, ASCE, **103**(7), pp. 757-768, 1977.

[16] Sengara, I.W., *Site Specific Seismic Study*, RFCC Cilacap Engineering Project, Cilacap, 2012. Unpublished.

[17] Abrahamson, N.A. & Silva, W.J., *Empirical Ground Motion Models,* report prepared for Brookhaven National Laboratory, New York, NY, 1996.

[18] Seed, H.B. & Idriss, I.M., *Simplified Procedure for Evaluating Soil Liquefaction Potential,* Journal of the Soil Mechanics and Foundations Division, ASCE, **107**(SM9), pp. 1249-1274, 1971.

[19] PT Pertamina, *CAP Design Report Area 8 RX-RG Tower*, RFCC Project, Pertamina RU-IV, Cilacap, Report No. RFCC-A-CV-RP-018, 2012. Unpublished.

[20] Team for Indonesian Seismic Map 2010 Revision, and Team for Ground Response Development and Risk Coefficient*, Indonesian Seismic Zoning Map, Indonesian Design Spectra,* Ministry of Public Works, http://puskim.pu.go.id/Aplikasi/desain_spektra_indonesia_2011/, July 2010. (Text in Indonesian).

[21] Ashford, S., Rollins, K., Bradford, S., Weaver, T. & Baez, J., *Liquefaction Mitigation Using Stone Columns Around Deep Foundations: Full-Scale Test Results*, Journal of the Transportation Research Board, **1736**, Paper No. 00-1408, pp. 110-118, 2000.